Development of a ratcheting, tension-only fuse mechanism for seismic energy dissipation

2015 NZSEE Conference

J. Cook[1], G.W. Rodgers[1], G.A. MacRae[2] & J.G. Chase[1]

[1]*Departments of Mechanical Engineering, University of Canterbury, Christchurch, New Zealand*

[2]*Departments of Civil and Natural Resources Engineering, University of Canterbury, Christchurch, New Zealand*

ABSTRACT: Seismic damage-resistant structures, such as jointed precast connections and rocking wall structures, usually require supplementary energy dissipation devices to limit peak displacements. Yielding steel fuses or buckling restrained braces (BRBs) can provide energy dissipation but have a tendency to create residual compressive forces after joint closing that can resist the re-centring of the structure and fight the post-tensioning forces on subsequent cycles. A ratcheting, tension-only fuse device has been developed to offer resistance to loading in tension, while offering negligible resistance to compressive motion. This lack of compressive forces allows re-seating of a rocking connection to minimise residual structural displacements. Upon re-loading, fuse engagement will be more rapid due to the ratcheting mechanism, as the absence of residual compressive loads reduces the amount of elastic take-up before yielding occurs. A prototype ratcheting fuse mechanism with a yield force of 45kN and an ultimate tensile force of 65kN has been designed and experimentally tested. The design was refined to provide ease of manufacture, eliminating complex and expensive processes, to reduce the overall construction costs. Experimental proof-of-concept testing on six fuse elements demonstrated the function of the ratcheting mechanism and assessed the hysteretic behaviour of the fuse element and the overall device with two different tooth pitch sizes. High speed camera footage of the ratcheting mechanism was recorded to assess engagement timing.

1 INTRODUCTION

The capital cost of the Canterbury earthquakes of 2010 and 2011 has been estimated to be as high as $40 billion (NZ Treasury 2014). The extent of the damage caused and the disruptions to the operation of facilities has resulted in an increase of public expectations regarding the resilience of structures to earthquake loading. Low damage structural technology is a large field covering much of the work that is being completed as engineers work towards improving building performance levels following seismic events (CERC 2012).

A key concept in such technology is the idea of providing specific energy dissipation mechanisms to absorb earthquake energy and reduce the damage to a structure. Supplementary energy dissipation is commonly provided for structures through the use of four broadly categorised types of dampers (Symans, et al. 2008). These dampers are viscous fluid dampers (Lee and Taylor 2001), viscoelastic solid dampers (Kanitkar, et al. 2006), yielding steel (Black, et al. 2004), and friction dampers, such as sliding hinge joints (Clifton 2005). A further category that is gaining interest is the use of extrusion dampers, such as the high force-to-volume (HF2V) lead-extrusion damper (Rodgers, et al. 2008).

Metallic dampers/yielding steel fuses remain a desirable option due to the familiarity of the behaviour of steel under loading, and their general simplicity in design. A key issue with some common approaches, such as with buckling restrained braces (BRBs), is the presence of residual compressive stresses after a seismic event. Such stresses limit the effectiveness of the device to allow the centring of a structure post-quake, and also impair their performance in a subsequent earthquake.

Slender bracing that yields in tension and buckles elastically in compression removes these residual compressive forces. However, plastic deformation on prior cycles will increase the unstressed member length and result in a dead-zone with take-up on subsequent cycles. Therefore, subsequent cycles will provide reduced energy dissipation capacity. An approach that has been conceived to address these issues is the use of a tension only, steel dissipation device, where dissipation may occur due to mechanisms such as yielding or friction. This concept was originally referred to as a Grip 'n' Grab (GnG) device and was modelled in a rocking system simulation (Gunning and Weston 2013). However, no design or experimental work has previously been completed for the particular concept. Other tension-only damper/bracing research has been conducted including with hysteretic dampers (Phocas and Pocanschi 2003) and seesaw systems (Kang and Tagawa 2012); however, the proposed device offers a novel alternative that aims to be a simple, cost-effective solution for industry.

2 DEVICE DESIGN

The GnG ratcheting, yielding fuse mechanism makes use of a linear ratcheting mechanism to achieve the desired single direction engagement. This mechanism allows the device to engage in tension, offering resistance to motion acting to displace a structure, while providing negligible impediment to any restoring motion. A number of concepts were considered for the ratchet mechanism including designs making use of friction-based or stepped interfaces. Particular attention was given to reliable engagement, low manufacturing cost and robustness of the design concepts. The initial chosen design is comprised of two pawls and a rack with teeth on both sides. A tension spring fitted between the pawls is used to aid initial engagement during tensile loading. Upon initial engagement the ratchet mechanism locks tighter as the engagement interface is self-stabilising and the tension spring provides initial engagement only. The two pawls rotate about pins located by a main support made from a standard RHS section. A circular yielding steel fuse element is attached to the rack, and each end of the device has a rectangular tongue for mounting in the MTS-810 test machine. Racks of two different pitch sizes, 20 mm and 40 mm, were built and tested. Figure 1 shows the assembly of the ratcheting mechanism.

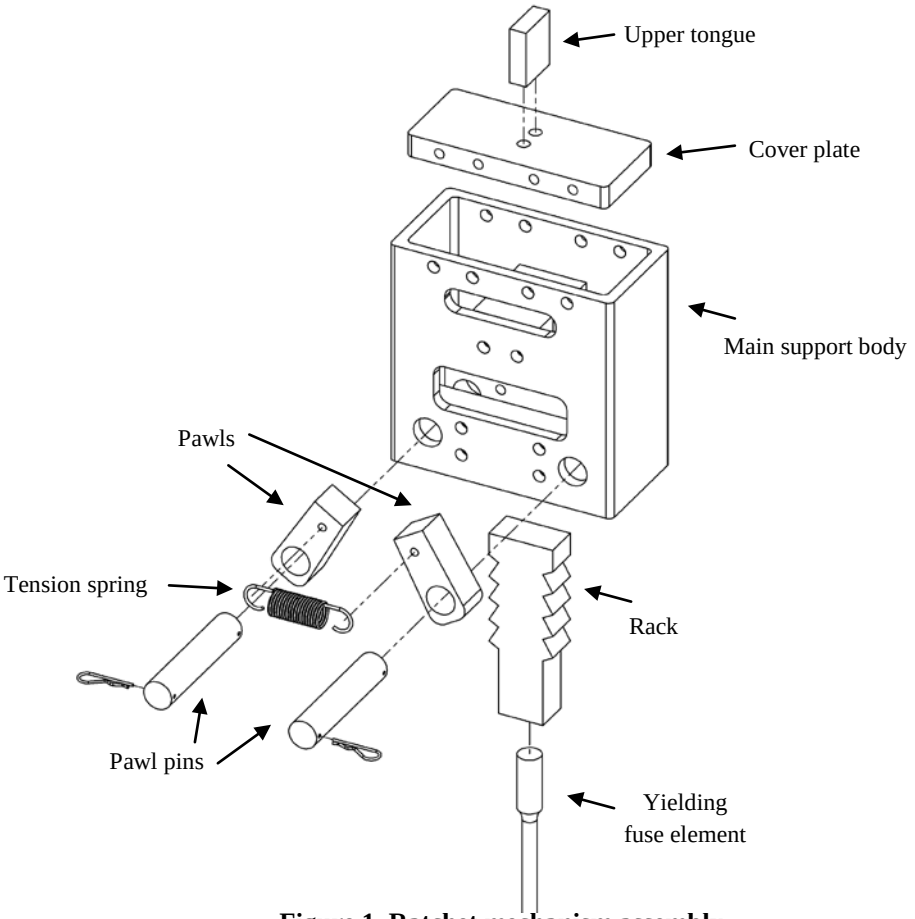

Figure 1. Ratchet mechanism assembly.

3 EXPERIMENTATION AND RESULTS

3.1 Test Apparatus

Experimental proof-of-concept testing on six fuse elements was used to demonstrate the function of the ratcheting mechanism and assess the hysteretic behaviour of the fuse element and the overall device. High speed camera footage of the ratcheting mechanism was recorded to assess engagement timing with the two different pitch sizes. A series of monotonic and cyclic tests were completed in an MTS-810 test machine using the setup shown in Figure 2.

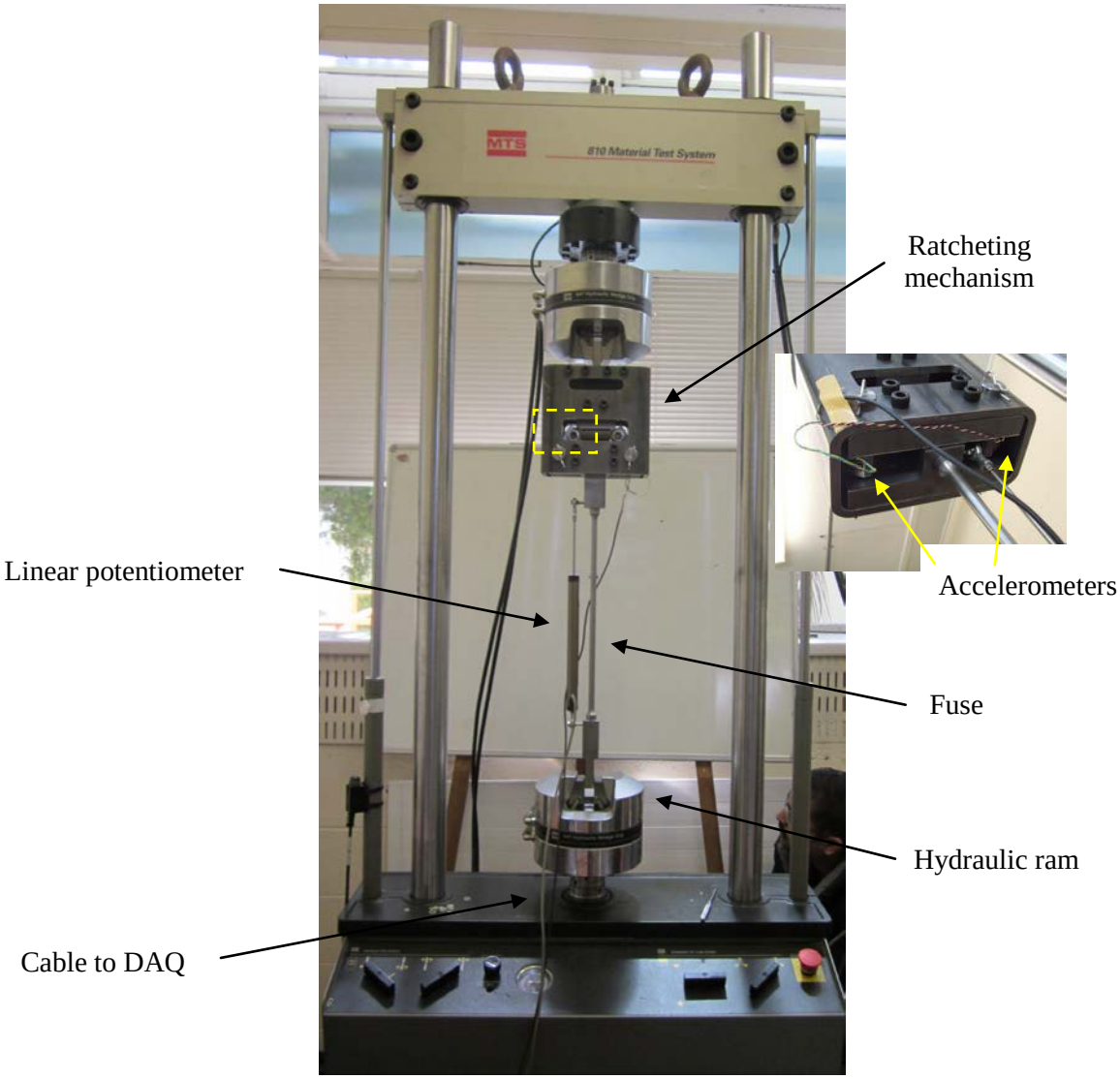

Figure 2. GnG prototype test apparatus (insert shows accelerometer placement). Inset box indicates close-up view in Figure 4.

3.2 Data acquisition

A data acquisition setup recorded five outputs against time during the experiments. The force and displacement of the hydraulic ram, at the lower end of the device, were recorded from the test machine (the upper crosshead remained stationary). A linear potentiometer position sensor was used to record changes in the length of the fuse element, and was mounted to the device via rod ends bolted to the lower region of the rack and the upper end of the lower tongue, as shown in Figure 2. The remaining two signals were taken from a pair of single-axis accelerometers mounted on the lower ends of the two pawls, shown in the insert in Figure 2. All data was sampled at 1000 Hz to ensure all frequencies were captured. High speed camera footage was recorded for several of the tests to measure pawl engagement time using a FASTCAM SA5 model 775K-C3 camera operating at 1000 fps.

3.3 **Monotonic testing**

Several tests of compressive monotonic loading were completed to characterise the ratcheting function of the device without yielding the fuse elements. During these tests the device was displaced in compression by 50 mm. This enabled the device to ratchet by two teeth when used with the 20 mm pitch rack, and one tooth when used with the 40 mm pitch rack, without yielding the fuse element. These tests were completed at different crosshead velocities and a summary of the monotonic testing is presented in Table 1, including the maximum compressive forces recorded.

Table 1. Summary of compressive monotonic testing.

Test No.	Rack Pitch (mm)	Velocity (mms^{-1})	Max. Compressive Force (kN)
M1	20	25	0.24
M2	20	25	0.47
M3	20	25	0.47
M4	20	50	0.48
M5	20	100	0.32
M6	20	50	0.76
M7	20	50	0.48
M8	40	50	0.72
M9	40	100	1.14

The maximum force experienced by the device during compressive loading, for any of the monotonic tests, was found to be 1.14 kN. This occurred during a test with the 40 mm pitch rack where the ram velocity was 100 mms^{-1}. This result fits with the expectation that slightly larger compressive forces would be experienced by the device during the use of the larger pitch rack. The larger teeth force the pawls to rotate slightly further outward, increasing the tension force in the spring which must be overcome for ratcheting to occur.

3.4 **Cyclic Testing**

Cyclic tests were also completed in order to assess the hysteretic behaviour of the fuse element and the overall device. A summary of the cyclic testing parameters is presented in Table 2 and results from this testing follow in Table 3. Due to the limited capacity of the prototype device, the cyclic tests with the 40 mm pitch rack were both completed in two sets of a single cycle in order to avoid interference of the rack with the top cover plate. Between cycles the springs were removed from the pawls, to allow the fuse subassembly to be moved back to its approximate original position before reassembly. Data recordings were zeroed prior to the second cycle and some reconstruction was required to obtain the effective force displacement figures.

Table 2. Summary of test parameters for cyclic testing.

Test No.	Rack Pitch (mm)	Amplitude (mm)	Frequency (Hz)	Cycles	Fuse Status
C1	20	30	0.5	3*	Fracture
C2	20	30	0.25	3	Fracture
C3	40	50	0.5	2	Fracture
C4	20	30	0.25	3	Intact
C5	20	30	0.25	3	Intact
C6	40	50	0.25	2	Fracture

*Initial machine overload limits meant that this test was interrupted after approximately one cycle before resuming to completion.

The maximum compressive force experienced by the device during any of the cyclic loading experiments was found to be 1.27 kN. This occurred during a test with the 40 mm pitch rack operating at 0.25 Hz. During the cyclic testing the two largest maximum compressive forces occurred during the two tests with the larger pitch rack. However, there was little difference (~8%) between the largest of the maximum compressive forces recorded for the smaller pitch experiments and the lower value for the two larger pitch experiments. In all tests the compressive forces are very low, as intended by design. The experimental values show a reasonable consistency, with an average yield force of 45.4 kN and an average ultimate tensile force of 65.8 kN. Hydraulic test machine limitations (maximum force of 100 kN) dictated the maximum fuse diameter used for this testing. The ratcheting mechanism is capable of much larger forces if required. Various dissipation methods, such as other variations of yielding steel fuses and friction connections, could be implemented with the ratcheting mechanism as required for specific applications. The average elongation to fracture was 70.8 mm. This represents ~ 79% of the expected 90 mm elongation at break according to approximate material properties from the MatWeb database. Therefore, the assumed uniform plastic strain throughout the entire fuse length may not have been obtained during testing.

Table 3. Summary of results of cyclic testing.

Test No.	Yield Force (kN)	Ultimate Tensile Force (kN)	Fuse Elongation to Fracture (mm)	Max. Compressive Force (kN)
C1	49.9	65.7	71.4	0.49
C2	42.4	65.1	65.2	0.30
C3	46.0	67.1	71.4	0.53
C4	43.5	65.3	>59.2*	0.35
C5	46.5	65.0	>59.3*	0.28
C6	44.1	66.7	75.2	1.27

*Samples did not fracture during test loading sequence.

4 HYSTERESIS BEHAVIOUR

The effect of the ratcheting mechanism produced a unique hysteresis loop for the behaviour of the system. A force displacement plot for the hydraulic ram of the test machine during the cyclic tests with the 20 mm pitch rack is presented in Figure 3. The start of the hysteresis loops are quite typical, displaying elastic behaviour, yielding and strain hardening before the first load reversal. After this point there is an elastic recovery region followed by a period where only negligible forces are experienced in compression. The bottom of the hysteresis loop lies essentially on the horizontal axis, indicating that little force is required for the unloading phase of the cycle.

Since the amplitude of the cyclic loading input exceeds the tooth pitch on the rack, the displacement at which the GnG device engages during the next loading cycle is reduced by an amount equal to the tooth pitch. This is shown in Figure 3 where it can be seen that during unloading of the initial cycle the displacement is approximately 13 mm after elastic recovery, and during the following cycle the elastic strain behaviour of the system is activated at a displacement of approximately -7 mm, with respect to the initial position. It is observed that similar behaviour occurs for the other two loading and unloading cycles, which demonstrate a completion of elastic recovery at a displacement of approximately 12.5 mm, and a resumption of elastic strain behaviour at a displacement of around -7.5 mm, with respect to initial position. Moreover, the hydraulic ram reaches a minimum position of ~-15 mm. Figure 3 indicates that up to 8 mm of free-travel exists before engagement of the rack and pawls. Similar behaviour was exhibited by the testing with the larger pitch rack, with some free-travel present upon reloading.

In Figure 3, it is shown that from a displacement of ~-15 mm to -7.5 mm, reloading occurs without much resistive force. This free-travel $x_{free\text{-}travel}$ is directly proportional to tooth pitch p and can be approximated by Equation 1 below (where it is assumed that $p < A < 2p$):

$$x_{free\text{-}travel} = A - p - \delta_{elastic} \quad (1)$$

where A is the amplitude of the displacement input cycle and $\delta_{elastic}$ is the elastic displacement recovered by the device during unloading, as shown on Figure 3. The engagement displacement values are consistent for tests with the same rack due to approximately equal starting positions, with the rack resting on the closed pawls.

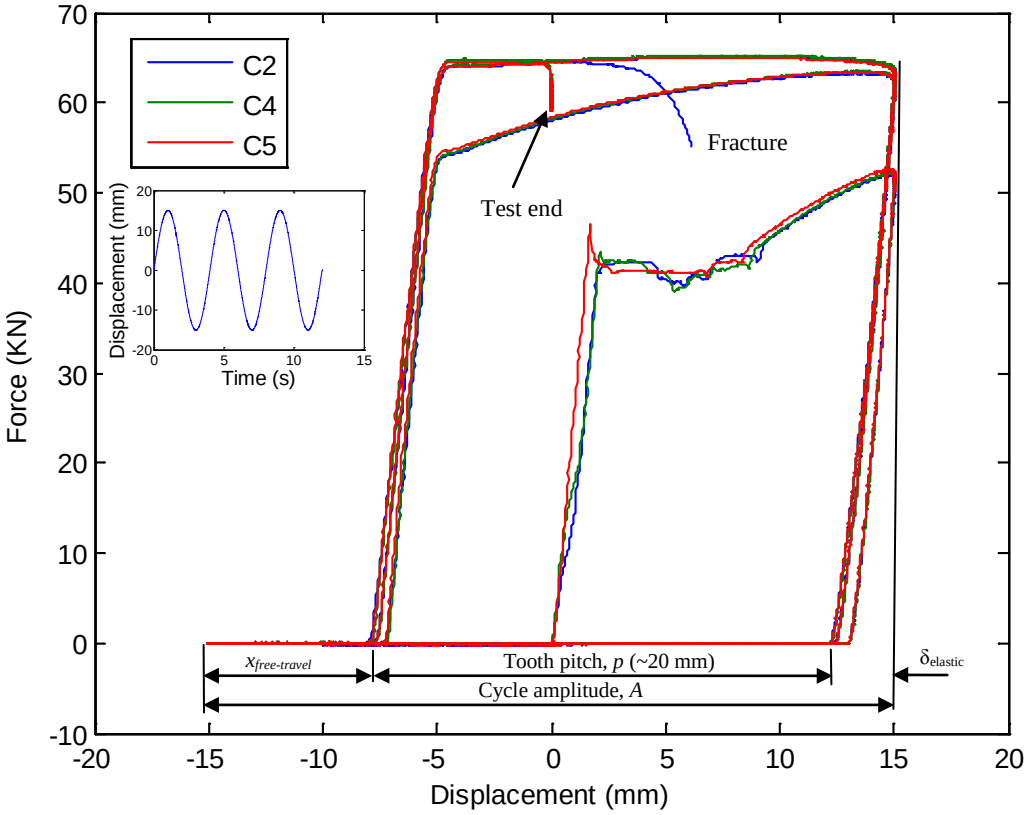

Figure 3. Force displacement hysteresis loops for cyclic testing of 20 mm pitch rack. The input displacement profile is inset.

This result differs from the expected behaviour of a regular yielding steel hysteresis loop due to the ratcheting mechanism essentially shifting the zero displacement datum. The amount of free-travel prior to re-engagement of the yielding mechanism on subsequent cycles is reduced as the displacement does not need to exceed that on prior cycles before energy dissipation can occur, as is a limitation with simple tension bracing. The onset of tensile yielding of the GnG device occurs when the force in the fuse exceeds the force at the start of the unloading phase in the previous cycle. While the test was cyclic, the material yields only in tension and the behaviour approximates a monotonic tensile test.

The benefit of a ratcheting system such as the GnG device is apparent in applications of seismic energy dissipation. In such applications the device could replace a traditional yielding steel device and reduce the take-up between loading cycles, resulting in more rapid engagement of the energy dissipation system. This faster response will reduce shock/impact loads and maximise the amount of energy absorbed by the device, thus minimising the response of the structure and the effects of such loading. It should be noted that a smaller tooth pitch will reduce the amount of free-travel and magnitude of any impact loading, but increase plastic displacement demand in the fuse element. As with traditional steel fuses, the total displacement capacity of the GnG device is limited by the available plastic displacement of the fuse prior to fracture. Variation in size and design of the fuse can

provide greater displacement capacity to suit specific applications.

5 RATCHETING MECHANISM BEHAVIOUR

The high speed camera footage was used to find the closure time for the ratcheting mechanism during the tests. This is defined as the time for the pawls to regain contact with the rack following the occurrence of ratcheting, and was determined by visual inspection of the high speed camera footage. Figure 4 shows a number of frames from the M9 monotonic test demonstrating the closure of a pawl with time stamps from the processing software. Each frame is 1 ms apart. A summary of the ratcheting mechanism behaviour is provided in Table 4.

Table 4. Summary of ratcheting mechanism behaviour.

Test No.	Individual pawl closure time (ms) [left, right]	Total closure envelope (ms)
M2	[**6**, 8] [**7**, 9]*	20, 29
M3	[**6**, 8] [**6**, 11]	14, 34
M4	[**6**, 10] [**6**, 9]	41, 42
M5	[**5**, 7] [**5**, 7]	22, 16
M7	[**5**, 13] [**5**, 13]	21, 33
M9	[8, **8**]	9
C2	[**6**, 11] [**5**, 12] [11, **6**]	18, 33, 20
C6	[**7**, 9] [11, **7**]	14, 13

*Bold font indicates lead pawl. For some tests multiple ratcheting actions occurred.

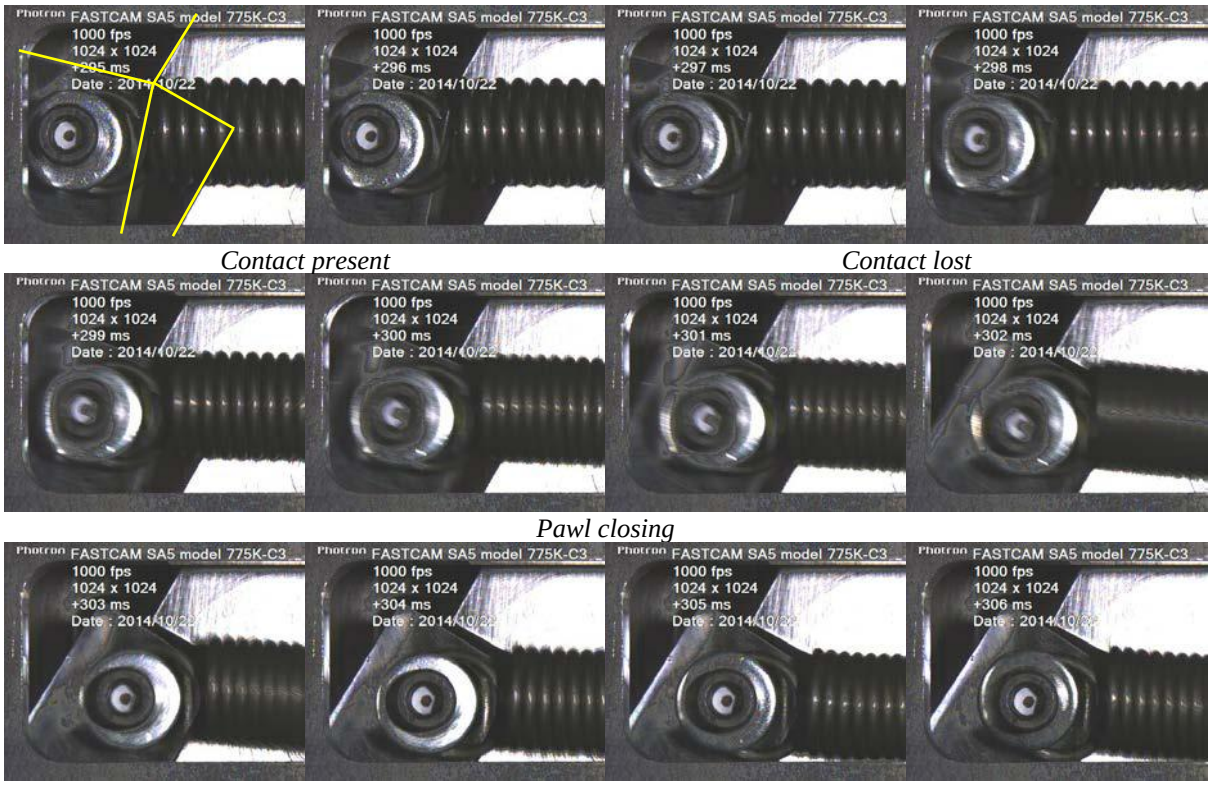

Figure 4. Closure of pawl captured by high speed camera during M9 monotonic test (where each frame is 1 ms apart). The outline of the pawl and rack are highlighted in the first image for clarity, as they are partially obscured by the spring. The section of the device shown here is indicated in Figure 2.

It was observed that in general the two pawls did not act perfectly in unison, with the ratcheting action of one of the pawls lagging slightly behind the other. This delay is likely due to imperfect symmetry of the pawl positions and the spring. The individual pawl closure time represents the time while contact with the rack is lost as the pawl rotates inward before contact is re-established, while the total closure envelope describes the time from the beginning of closure for the lead pawl to the end of closure for the lagging pawl. The largest total closure envelope was found to be 42 ms. This period of time corresponds to a maximum ram displacement of approximately 4.2 mm during the test involving the fastest ram movement rate of 100 mms^{-1}. This time also represents around 2-4% of the expected 1-2 s period for many common structures. The smallest closure envelope recorded, 9 ms, is representative of a ram displacement of 0.90 mm at the fastest ram speed used in testing, and approximately 1-2% of the expected period for structures of the same size. With careful design, reloading during the small window where only one pawl is engaged will not prevent tensile load carrying and energy dissipation capacity.

6 CONCLUSIONS

A ratcheting, tension-only fuse device has been developed to offer resistance to loading in tension, while offering negligible resistance to compressive motion. This lack of compressive forces allows re-seating of a rocking connection and minimises residual structural displacements. Upon reloading, fuse engagement will be more rapid than a simple steel fuse due to the ratcheting mechanism, as the absence of residual compressive loads reduces the amount of elastic take-up before yielding occurs. Moreover, in post-tensioned rocking systems residual compressive forces partially offset the clamping effect of the post-tensioning. Therefore, the overall resistance to the onset of rocking may be reduced for subsequent cycles using a traditional yielding steel component such as a BRB. The GnG device eliminates this effect for consistent, repeatable rocking behaviour.

Continuing work on this project is focused on the testing of a second, axisymmetric design with a reduced tooth pitch. A hysteresis model has been developed to capture the behaviour of the ratcheting fuse mechanism and is being used to assess the cumulative displacement demand on the fuse during a range of earthquake inputs. The work is progressing toward recommendations for the implementation of the GnG device to full-scale structures.

7 ACKNOWLEDGEMENTS

Financial support for the experimental work from the BRANZ Building Research Levy is gratefully acknowledged, as well as The Sir Robertson Stewart Scholarship and the support of the UC Quake Centre.

8 REFERENCES

Black, C.J. Makris, N. & Aiken, I. 2004. Component testing, seismic evaluation and characterization of buckling-restrained braces, *Journal of Structural Engineering*, 130(6): 880-894

Canterbury Earthquakes Royal Commission. 2012. *Low-damage Building Technologies*. Christchurch, New Zealand.

Clifton, G.C. 2005. *Semi-rigid joints for moment-resisting steel framed seismic-resisting systems*, PhD Thesis, The University of Auckland, Auckland, New Zealand.

Gunning, M. & Weston, D. 2013. *Assessment of Design Methodologies for Rocking Systems*, ENCI493 Report, Supervised by MacRae, G.A., Department of Civil and Natural Resources Engineering, University of Canterbury, Christchurch, New Zealand.

Kang, J.D. & Tagawa, H. 2013. Seismic response of steel structures with seesaw systems using viscoelastic dampers. *Earthquake Engineering and Structural Dynamics*, 42(5): 779-794

Kanitkar, R. Aiken, I.D. Nishimoto K. & Kasai, K. 2006. Viscoelastic dampers for the seismic retrofit of buildings: An overview of advancements in viscoelastic materials and analytical capabilities, Paper No. 1299, *Proc. 8th U.S. National Conference on Earthquake Engineering, EERI, Oakland, Calif., 18-22 April, 2006*

Lee, D. & Taylor, D.P. 2001. Viscous damper development and future trends, *Structural Design of Tall Buildings,* 10(5): 311-320

New Zealand Treasury. 2014. *2014 Budget: Budget Policy Statement.* Wellington, New Zealand

Phocas, M.C. & Pocanschi, A. 2003. Steel frames with bracing mechanism and hysteretic dampers. *Earthquake Engineering and Structural Dynamics,* 32(5): 811-825

Rodgers, G.W. Solberg, K.M. Chase, J.G. Mander, J.B. Bradley, B.A. Dhakal, R.P. & Li, L. 2008. Performance of a damage-protected beam-column subassembly utilizing external HF2V energy dissipation devices, *Earthquake Engineering and Structural Dynamics*, 37(13): 1549-1564.

Symans, M.D. Charney, F.A. Whittaker, A.S. Constantinou, M.C. Kirhcer, C.A. Johnson, M.W. & McNamara, R.J. 2008. Energy dissipation systems for seismic applications: Current practice and recent developments, *Journal of Structural Engineering*, 134(1): 3-21.